Supporting Information

Mechanical Model of Globular Transition in Polymers

Simon Tricard,*[a] Robert F. Shepherd,[a] Claudiu A. Stan,[a] Phillip W. Snyder,[a] Rebecca Cademartiri,[a] Danny Zhu,[a] Igor S. Aranson,[b] Eugene I. Shakhnovich,[a] and George M. Whitesides[a]

[a] Dr. S. Tricard, Dr. R. F. Shepherd, Dr. C. A. Stan, Dr. P. W. Snyder,
Dr. R. Cademartiri, D. Zhu, Prof. E. I. Shakhnovich, Prof. G. M. Whitesides
Department of Chemistry and Chemical Biology
Harvard University
12 Oxford Street, Cambridge, MA 02138 (USA)
E-mail: simon.tricard@insa-toulouse.fr
[b] Dr. I. S. Aranson
Argonne National Laboratory
9700 South Cass Avenue, Argonne, IL 60439 (USA)

Experimental Section

Materials. Nylon-6,6 rods with a diameter of 6 mm and acrylic spheres with a diameter of 3 mm were purchased from McMaster-Carr Supply Company. We cut the rods into 14 mm-long cylinders. Holes with a diameter of 1.3 mm were drilled through the spheres and the cylinders. 6-mm wide transparent acrylic spheres were purchased from Engineering Laboratories. The aluminum honeycomb panel was purchased from Home Depot. Silver-coated, 2 × 2-mm crimp beads were purchased from Beadalon. Nylon-6,6 threads with a diameter of 75-µm and 600-µm were purchased from thethreadexchange.com. Fadeless® paper was purchased from Pacon Corporation. Magnetic hematite 3 × 9-mm tubes were purchased from Arizona Bead Company. To stain the transparent nylon cylinders blue, we immersed them in an aqueous solution of Disperse Blue 14 and placed on a hot plate at a temperature of 100 °C for 30 min. Dyed cylinders were washed with water and ethanol and dried with a N_2 stream.

Construction and Agitation of a Large Flat Surface. The flat surface on which the objects were agitated (1.2×1.2 m square, ~7 kg weight) was made from an aluminum honeycomb panel and was supported from the ceiling via an elastic cord joined to four cables which were anchored to the corners of the panel. The distance between the plate and the attachment point to the ceiling was 1.3 m. We attached to the center of the plate, below it, a pendulum made from a light (~0.1 kg) 0.3-m rigid rod with an end weight with a mass of 1.4 kg. The pyramid defined by the panel and the cables was wrapped in a polyvinyl chloride (PVC) film to control the humidity above the plate.[14] We maintained a relative humidity higher than 60% using an air humidifier (Vicks V5100NS). To record snapshots of the system during agitation, we used a photo camera (Nikon D40) that was suspended ~1 m vertically above the plate. To achieve pseudo-random agitation,

we applied two shaking drives: one from an orbital shaker attached to the plate, and one from a linear actuator which kicked the weight of the pendulum under the plate. The orbital shaker (Madell Technology Corp., ZD-9556-A) was attached to the plate via an elastic polyurethane cord, and the motion it imparted to the plate was a combination of orbital translation with a small-amplitude angular oscillation. The radial amplitude of the orbital shaker was 5.1 mm, and its frequency was variable; we used orbital frequencies ranging from f = 80 to f = 150 revolutions per minute (rpm). The second shaking motion had the role of randomizing the orbital motion. We kicked with a linear actuator (LinMot, Inc., P01-23x80) the weight under the plate; the linear actuator moved at a fixed frequency of 4 Hz in all experiments, but the times at which it impacted the pendulum were not periodic due to the complicated motion of the pendulum. The frequency of kicks was higher than the frequency of orbital shaking, and the system did not complete a full orbit between kicks to the pendulum. The overall motion of the plate was aperiodic but not entirely random, and we estimated that the maximum horizontal acceleration of the plate was approximately 5 m/s^2. The area of agitation of the components (spheres and cylinders-on-a-string) was defined by an aluminum rim with a diameter of 0.48 m. We covered the surface of the board with paper to control the movement of the spheres and the cylinders; the roughness and softness of the paper was such that the objects consistently rolled but did not slide.

Preparation of the Cylinders-on-a-string. The flexible links in the chain were weakly elastic and were made from a nylon string on which we strung three 3.18-mm diameter PMMA spheres. Aluminum crimps fixed the cylinders on the string and controlled the elasticity of the chain, as described previously.[12-14] We chose a system of ten cylinders with a contour length L = 23.9 cm. For the non-magnetic chain, we used a Nylon-6,6 threads with a diameter of 75 μm and Nylon cylinders. The persistence length was previously determined and was equal to L_p = 12.2 cm.[12]

When we used several chains, the system jammed in few minutes – because of a high number of inelastic collisions, which are known to lead to clustering.[26] For the magnetic chain, we kept the same sequence, but we chose a Nylon-6,6 thread with a diameter of 600 μm and magnetic cylinders. To fabricate the magnetic cylinders, we enlarged the holes of the Nylon cylinders to a diameter of 3.2 mm and glued hematite tubes inside with epoxy glue.

Image Analysis. Two different designs of colors have been used. For the study with the non-magnetic cylinders, we used a white paper background and gray cylinders-on-a-string; we stained cylinders at the termini to increase the visual contrast between the middle cylinders of the chain and the cylinders at the ends of the chain and to facilitate image analysis. For the study with the magnetic cylinders we dyed all the cylinders in blue and used a brown paper background; this choice of colors improved the reliability of the image analysis. The free acrylic spheres are transparent in both cases but appeared white on the images because of the reflection of the light from the flash of the camera. We observed the evolution in time of the radius of gyration of the chain by collecting one picture of the system under continuous agitation. We adapted the time of measurements to the frequency of agitation, so that the chain probed all the possible conformations: every 1 min for f = 80 rpm to 100 rpm, every 30 s for f = 110 rpm to 130 rpm, and every 20 s for f = 140 rpm and 150 rpm. All experiments were started in an extended conformation, but we waited until the system reached a steady state before recording images. We collected data only when the system could freely evolve and explore all the possible conformations, *i.e.* when the system was not jammed because of a too high FR or a too low f. The radius of gyration was calculated averaging results form 100 pictures.

The radius of gyration of the chain was determined with custom-made script developed in Java that analyzed each frame separately. The script used a sequence of threshold operations,

erosions, dilations, and removal of small-area signals to produce monochrome images that preserved only the image of the cylinders; from such images, the position of the end cylinders and the center-of-mass of the chain can be computed automatically. The details of the operations in the sequence were optimized separately for the two types of chains used (magnetic and non-magnetic), resulting in two distinct image-processing procedures. In both cases, since the processes were not entirely reliable, each processed image was shown to a human viewer, with the detected cylinder center locations marked on the image. The viewer could then edit the locations if they were incorrect. This system allowed the cylinders to be detected more accurately and quickly, and with less work, than a purely manual system, while maintaining high accuracy. After the verification of the processed images, we calculated the radius of gyration from the coordinates of the centers of mass of the cylinders for each frame in the image sequence.

The error bars represent 95% confidence intervals in Figure 3a and Figure 5a. They represent the spread of frequency values in the area of overlap between 68.3% confidence intervals of the two linear fits whose intersection defines the phase transition frequencies f_0 in Figure 3b. The error bars correspond to the 95% confidence intervals of the sigmoidal fits in Figure 5b. In both Figures 5a and 5b, we only indicate the direction where $f_0(60\%)$ and $f_0(90\%)$ are located, as they are outside the range of frequencies investigated experimentally..

Figure S1. Histograms of the evolution of the distribution of the radii of gyration R_g of the chain, at different frequencies of the orbital shaker *f*, when the filling ratios of free spheres *FR* was increased: *FR* = 40% (a), 50% (b), 60% (c), 70% (d), 80% (e). In graphs (b) to (d), the plots at low *f* values (I) were separated from plots at high *f* values (II) for clarity; the average value of R_g increased with *f* in I, whereas it decreased in II. The lines connect experimental data.

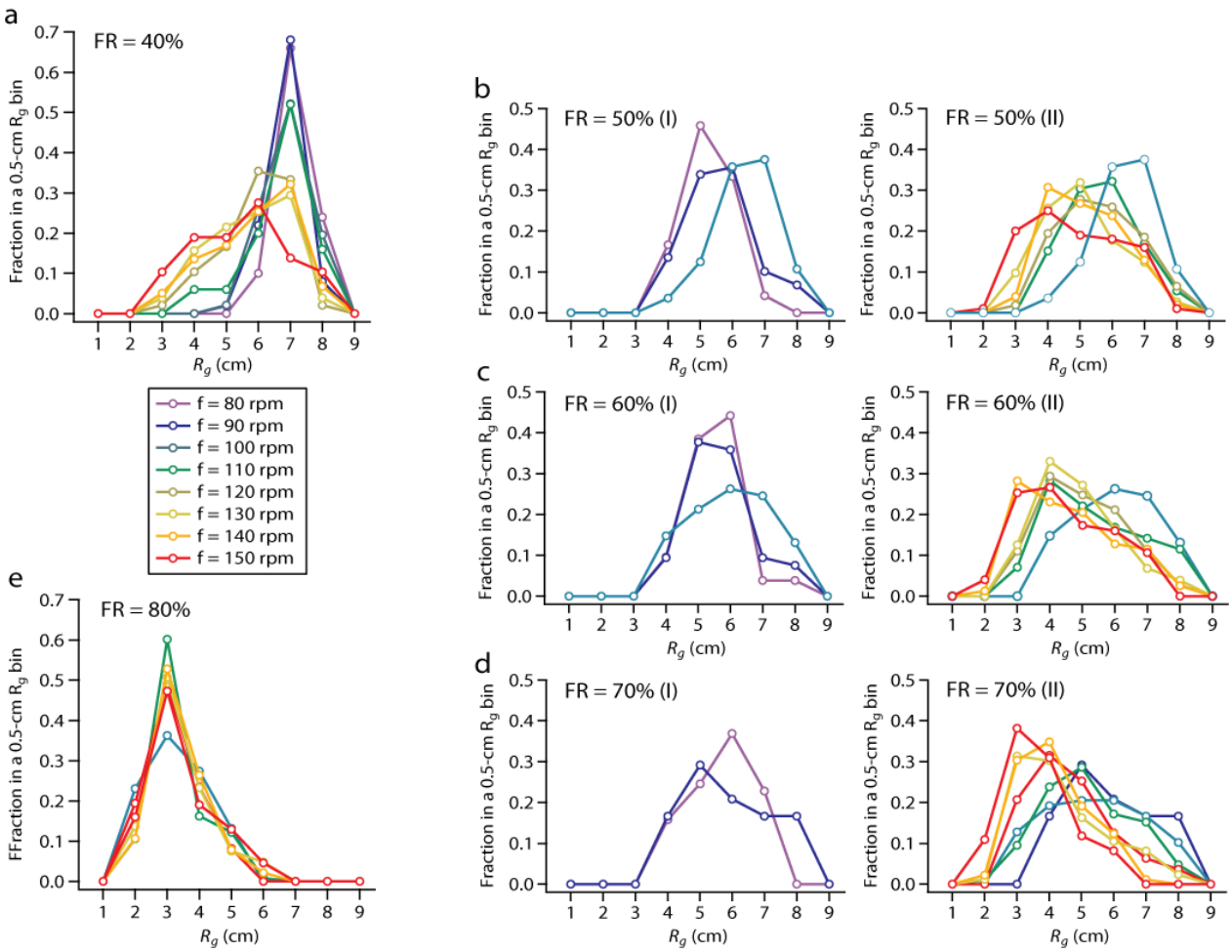

Figure S2. Histograms of the evolution of the distribution of radii of gyration R_g of the chain, at different frequencies of the orbital shaker *f*, when the filling ratio of free spheres *FR* was increased. The lines connect experimental data.